Analysis of Rotating Flow Around a Growing Protein Crystal

Daniel N. Riahi and Charles W. Obare

Department of Mathematics
University of Texas-Pan American
Edinburg, Texas 78541-2999 USA
driahi@utpa.edu

Abstract

We consider the problem of steady flow around a growing protein crystal in a medium of its solution in a normal gravity environment. The whole flow system is assumed to be rotating with a constant angular velocity about a vertical axis which is anti-parallel to the gravity vector. Convective flow takes place due to the solute depletion around the growing crystal which leads to a buoyancy driven flow. Such convective flow can produce inhomogeneous solute concentration, which subsequently generate non-uniformities in the crystal's structure finalizing lower quality protein crystal. Using scaling analysis within a diffusion boundary layer around the crystal, we estimate the magnitude of the convective flow velocity and other dependent variables of the flow system for cases of weak, moderate and strong rotation and either strong or weak buoyancy. We find, in particular, that for moderate rate of rotation, convective flow is weakened significantly as the rotation rate increases. This result may be of interest for production of high quality protein crystal since the effect of the convective flow around the growing protein crystal is found to be weakened significantly by the rotational constraint.

1. Introduction

A large number of experiments on earth and in space involving protein crystal growth have been carried out in the last two decades or so, including those more recent ones due to Cang et al. (2003), Moreno et al. (2007) and Heijna et al. (2008). Some of the space experiments under microgravity have been able to produce some types of crystals that were relatively larger and better ordered than those grown on earth under normal (earth) gravity condition [Day and McPherson (1992), Long et al. (1994)]. The main reason for growing protein crystals in space

has been to achieve diffusion controlled growth conditions, which was considered to produce higher quality crystal. However, there have been also a number of flight experiments that yielded crystals with no improvement in the quality and internal order just like those low quality crystals, which were grown under the normal gravity condition and in the absence of rotational constraint. One problem for the growing protein crystal in space can be the undesirable effects of impulsive disturbances from large thruster firings due to shuttle operations, which can adversely affect the concentration field near the crystal face.

However, there have been some experiments in centrifuge [Blagova et al. (1997)] for growing some types of protein crystals, like Uridine Phosphorylase (Uph), which indicated production of larger and higher quality crystals under the influence of a rotational constraint. Crystallization of larger size of Uph has become suitable for x-ray analysis. In addition, Uph has been identified as the enzyme that is also responsible for the cleavage of some pyrimidine nucleoside analogs, possessing anti-tumor activity [Blagova et al. (1997)].

Ramachandran et al. (1995) carried out studies of solutal convection in protein crystal growth under both normal and low gravity conditions and in the absence of rotation. For steady flow, they found, in particular, that their analytical solutions based on some approximate methods, provided useful information about the flow velocity and mass transport in the vicinity of a growing cylindrical protein crystal.

Lee and Chernov (2002) studied buoyancy driven axisymmetric convection during protein crystallization and in the absence of rotation. They considered more realistic boundary conditions for the protein solution at the crystal face and included the presence of impurity in the liquid. They carried out some scaling analysis [Barenblatt (1996)] for the flow within a boundary layer around a spherical protein crystal and determined, in particular, some estimation of the strength of convection against that of diffusion. In addition, they obtained results for axisymmetric flow around a cylindrical protein crystal, which were based on full-scale numerical simulations of the governing equations and were independent from those based on the scaling analysis, and found good agreements with the related results based on their scaling analysis of flow around the spherical protein crystal.

In the present investigation we carry out scaling analysis [Barenblatt (1996)] of the type used before by Lee and Chernov (2002) and by Worster (1991) and Riahi (2001) in other fluid flow problems. Such analysis is a useful tool often used for simplifying the governing equations which can be lengthy such as those encountered in the fluid mechanics. In such analysis the leading terms in the equations are identified and retained, and all the rest of the smaller terms in the equations are ignored and dropped from the equations. Then, the leading order results for the dependent variables and other quantities are determined, which are based on the leading terms that were retained in the equations. For the axisymmetic flow around a growing spherical protein crystal and in the absence of rotation, such scaling analysis was carried out by Lee and Chernov (2002), but here we apply such analysis for a more realistic case of non-axisymmetric flow around such growing protein crystal and in the presence of an external constraint of rotation. The applied scaling analysis used here can also be thought as an asymptotic analysis [Zeytounian (2004)] in the limit of either sufficiently large axial flow (strong buoyancy) or sufficiently small axial flow (weak buoyancy). We found interesting results. In particular, we found that presence

of an intermediate rotation rate is beneficial in the sense that the flow velocity near the crystal face is weakened as the magnitude of the rotation rate increases.

2. Governing System

We consider the problem of a protein crystal growing in a cylindrical chamber containing the solution. Such crystal will obviously grow until no more protein is available in the solution. However, since the protein crystal is much smaller in size than the volume of the solution, a steady solution of the governing equations can be attained to the leading order terms after an initial phase of flow adjustment around the growing crystal.

We consider a spherical protein crystal of radius h, in the central part of the container of its solution under a normal (Earth) gravity environment (Figure 1). We assume the whole flow system is rotating about the vertical axis z, which is anti-parallel to the force of gravity, with a uniform rotation rate Ω, and the governing equations for the flow are assumed in a coordinate system which is rotating with the flow at such rotation rate and direction.

The governing equations are the continuity equation for incompressible fluid flow, the momentum equation under Boussinesq approximation [Chandrasekhar (1961)] for the flow velocity vector and the concentration equations for the protein and impurity. It turns out to be sufficient to consider the governing equations in cylindrical coordinate, where the Laplacian operator is given by

$$\nabla^2 \equiv \left(\frac{1}{r} \frac{\partial}{\partial r} \left(r \frac{\partial}{\partial r} \right) + \frac{1}{r^2} \frac{\partial^2}{\partial \theta^2} + \frac{\partial^2}{\partial z^2} \right),$$

which is in cylindrical frame (r, θ, z). Here r and θ are the radial and azimuthal variables, respectively, and z is the axial variable whose axis coincides with the vertical axis. The continuity equation is

$$\frac{1}{r} \frac{\partial}{\partial r}(ru) + \frac{1}{r} \frac{\partial v}{\partial \theta} + \frac{\partial w}{\partial z} = 0. \tag{1a}$$

The radial, azimuthal and axial components of the momentum equation are

$$\frac{\partial u}{\partial t} + u \frac{\partial u}{\partial r} + \frac{v}{r} \frac{\partial u}{\partial \theta} - \frac{v^2}{r} + w \frac{\partial u}{\partial z} = -\frac{\partial p}{\partial r} + \nu \nabla^2 u - \frac{u}{r^2} - \frac{2}{r^2} \frac{\partial v}{\partial \theta} + 2\Omega v + [\frac{\rho_1}{\rho_1^0}]r \cos^2 \theta \Omega^2, \tag{1b}$$

$$\frac{\partial v}{\partial t} + u \frac{\partial v}{\partial r} + \frac{v}{r} \frac{\partial v}{\partial \theta} + \frac{uv}{r} - w \frac{\partial v}{\partial z} = -\frac{1}{r} \frac{\partial p}{\partial \theta} + \nu (\nabla^2 v - \frac{v}{r^2} + \frac{2}{r^2} \frac{\partial u}{\partial \theta})$$
$$- 2\Omega u - [\frac{\rho_1}{\rho_1^0}]r \cos \theta \sin \theta \Omega^2, \tag{1c}$$

$$\frac{\partial w}{\partial t} + u\frac{\partial w}{\partial r} + \frac{v}{r}\frac{\partial w}{\partial \theta} + w\frac{\partial w}{\partial z} = -\frac{\partial p}{\partial z} + \nu\nabla^2 w - g[\rho_1\gamma],$$ (1d)

where it is assumed that there is only slight amount of contamination due to the impurity concentration, so that the buoyancy term due to the impurity is neglected in (1d). The concentration equations for protein ρ_1 and impurity ρ_2 are

$$\frac{\partial \rho_1}{\partial t} + u\frac{\partial \rho_1}{\partial r} + \frac{v}{r}\frac{\partial \rho_1}{\partial \theta} + w\frac{\partial \rho_1}{\partial z} = D_1\nabla^2\rho_1$$ (1e)

and

$$\frac{\partial \rho_2}{\partial t} + u\frac{\partial \rho_2}{\partial r} + \frac{v}{r}\frac{\partial \rho_2}{\partial \theta} + w\frac{\partial \rho_2}{\partial z} = D_2\nabla^2\rho_2.$$ (1f)

Here u, v and w are the radial, azimuthal and axial components of the flow velocity vector $\mathbf{u}$, respectively, ν is the kinematic viscosity, p is the modified pressure (pressure divided by ρ_1^0), γ is the protein solutal expansion coefficient, g is the acceleration due to gravity, D_1 and D_2 are the coefficients of the solutal diffusivity for the protein and impurity, respectively, and ρ_1^0 is the initial uniform concentration of the crystallizing protein.

The boundary conditions at the crystal surface are [Lee and Chernov (2002)]

$$D_1\frac{\partial \rho_1}{\partial n} = \rho_1^c V = \beta(\rho_1 - \rho_1^c), \quad D_2\frac{\partial \rho_2}{\partial n} = (K-1)\rho_2 V, \quad K \equiv \frac{\rho_2^c}{\rho_2}, \quad u = v = w = 0,$$ (2a-c)

where β (cm/s) is the kinetic coefficient, which characterizes the rate at which molecules are incorporated by the growing protein crystal, V is defined in (2a), and n is the normal distance along the axis pointing into the liquid from the crystal face.

The boundary conditions at the container surface are

$$u = v = w = \frac{\partial \rho_1}{\partial n} = \frac{\partial \rho_2}{\partial n} = 0.$$ (2d)

It should be noted that the main mathematical difference between the present model and that due to Lee and Chernov (2002) is that the present model treats non-axisymmetric system subjected to an external constraint of rotation, while the model of Lee and Chernov (2002) was for the simpler case of non-rotating axisymmetric system.

3. Analysis and Results

Consider a spherical protein crystal of radius h in the medium of its solution under a normal gravity condition. At initial time $t = 0$, the uniform density of solution is ρ^s, and the uniform concentrations of the crystallizing protein and impurity are denoted by ρ_1^0 and ρ_2^0, respectively. For $t > 0$, the concentrations are non-homogeneous and non-uniform in general and are denoted by ρ_1 and ρ_2. Crystal-solution equilibrium is reached when $\rho_1 = \rho_1^e$. Inside the protein crystal, the densities for the protein and impurity are designated by ρ_1^c and ρ_2^c. We consider the fully nonlinear regime but for weakly non-axisymmetric case, where the flow dependence are assumed to vary weakly with respect to the azimuthal variable θ. For strong buoyancy driven flow, which implies strong convection, the Peclet number $P_r = wh/D_1$, which is a non-dimensional parameter representing the axial flow, is large ($P_r \gg 1$), while for weak buoyancy driven flow P_r is small ($P_r \ll 1$) [Lee and Chernov (2002)]. The present scaling analysis can be thought as an asymptotic analysis in the limits of either very large P_r (strong buoyancy) or very small P_r (weak buoyancy).

3.1. Convection Versus Diffusion

Following Lee and Chernov (2002), we first focus on convection versus diffusion aspect. We compare four velocities involved in the system. These are the flow rate w (in the axial direction), diffusion rate D_1/h, kinetic coefficient β and the crystal growth rate V. The flow rate w can be large or small depending on the order of magnitude of the buoyant force. For sufficiently low gravity case, diffusion dominates and so it is reasonable to put w aside. Protein crystal growth is slow, so that β at the crystal-solution interface is typically lower than the diffusion rate D_1/h, at which molecules are transported through the solution to the surface. Since β is typically small, we are interested here in high super-saturation, where $\rho_1^0 \gg \rho_1^e$.

Now, from (2a), we have $V \approx \beta \rho_1 / \rho_1^c \approx \beta \rho_1^0 / \rho_1^c \ll \beta$ at the interface because $\rho_1^0 \ll \rho_1^c$. Thus, we have $D_1 / h > \beta \gg V$. If V is so small that $v > V$, then the problem can be treated as a purely diffusion one because V is of order $10^{-8} cm/s$ and can hardly stir up convection. Problem is about a crystal growing in a finite isolated body of solution. So crystal will grow until no more protein is available. Since crystal $\ll$ volume of solution, a steady state is attained after an initial phase of adjustment of solution around crystal long before protein solute is significantly depleted.

3.2. The Case of Weak Rotation and Strong Buoyancy

We consider the case where convection occurs due to the solute depletion around the growing crystal leading to a decrease in density by an amount denoted by $\Delta\rho^s$ and a resulting buoyant force of $g\Delta\rho^s$. In an assumed leading order steady state, the buoyant force and the opposing viscous force convert the depleted region into a diffusion boundary layer of thickness δ. For the momentum equation and within this boundary layer, diffusion of vorticity, represented by

viscous terms, is important and dominates to leading term over the nonlinear inertial terms in the assumed steady state. For sufficiently small rotation rate, the centrifugal force, which contains a factor of Ω^2, is small in comparison to the Coriolis force, which contains a factor of Ω. Comparing the Coriolis force with the leading term of the viscous force in (1b) or (1c), we obtain the condition

$$2\Omega << \nu/\delta^2, \tag{3}$$

which is valid when rotation is weak. Thus, the rotational constraint here has at most minor effects and will not enter the leading order balance of forces which determine the flow rate. In this paper, when rotation is weak, we obtain the leading expression for the axial velocity, which is the main component of the velocity vector, from the axial component (1d) of the momentum equation. The equation (1d) then yield the following leading balance

$$\nu \frac{w}{\delta^2} \approx g \frac{\Delta \rho^s}{\rho^s}, \tag{4a}$$

where

$$\Delta \rho^s = \omega(\rho_p - \rho_w)(n^s - n) = \rho^s \gamma(\rho_1^0 - \rho_1). \tag{4b}$$

Here, ω, ρ_w and ρ_p are the volume, density of water and density of a protein molecule, respectively, n^s and n are the number of protein molecules per unit volume in the ambient and at interface respectively , ρ_1 is evaluated at interface, and

$$\gamma = \left(\frac{1}{\rho^s}\right)\left(\frac{\partial \rho^s}{\partial \rho_1^0}\right)(\rho_p - \rho_w)/(\rho_p \rho^s).$$

The expression in the right-hand side in (4b) is due to the gravity term in (1d) and the hydrostatic approximation of the axial-derivative of the pressure term in (1d). From (2a) we find

$$D_1 = \left(\frac{\rho_1^0 - \rho_1}{\delta}\right) \approx \beta\left(\rho_1 - \rho_{1_w}^e\right),$$

which then yield

$$(\rho_1^0 - \rho_1) \approx \frac{\beta \delta}{D_1}(\rho_1^0 - \rho_1^e), \tag{5}$$

because $\beta \delta / D_1 << 1$ (on the basis of $\beta h / D_1 < 1$ and $\delta << h$) and $\rho_1^0 \approx 10^{-3}$ and $\rho_1^e \approx 2.35 \times 10^{-5}$ for Ferritin, as an example, so that $\rho_1^0 \approx \rho_1$, which we assumed initially. Thus, (5) follows.

Now, by diffusion alone, the boundary layer δ thickness grows like $\sqrt{D_1 t}$ .since balancing diffusion term with temporal derivative term in either (1e) or (1f) implies such result. When there is enough convection, δ reaches its limiting value when flow reaches a steady state. The axial flow rate w is assumed to be the dominant flow component that together with radius of the protein, determine the relevant t in $\sqrt{D_1 t}$. Thus,

$$\delta \approx \sqrt{D_1 t} \approx \sqrt{\frac{D_1 h}{w}} . \tag{6}$$

Now, using (4b) and (5)-(6) into (4a), we have

$$\gamma \frac{w}{\frac{D_1 h}{w}} \approx g\gamma\left(\frac{\beta}{D_1}\right)\left(\rho_1^0 - \rho_1^e\right)\sqrt{\frac{D_1 h}{w}} \quad \text{or} \quad w^{\frac{5}{2}} \approx \frac{g\gamma\beta}{\upsilon D_1}\left(\rho_1^0 - \rho_1^e\right)\left(D_1 h\right)^{\frac{3}{2}} \approx \frac{g\gamma\beta}{\upsilon}\left(\rho_1^0 - \rho_1^e\right)D_1^{\frac{1}{2}} h^{\frac{3}{2}} .$$

Thus,

$$w \approx \left[\frac{g\gamma\beta\left(\rho_1^0 - \rho_1^e\right)}{\upsilon}\right]^{2/5} D_1^{\frac{1}{5}} h^{\frac{3}{5}} . \tag{7}$$

Since $\rho_1^0 \gg \rho_1^e$, (6) becomes to the leading term

$$w \approx \left[\frac{g\gamma\beta\left(\rho_1^0\right)}{\upsilon}\right]^{2/5} D_1^{\frac{1}{5}} h^{\frac{3}{5}} . \tag{8}$$

The result given in (8) is obtained for the case of weak rotation and strong buoyancy driven flow.

3.3. Case of Weak Rotation and Weak Buoyancy

We now analyze the case where convection is dominated by protein diffusion since buoyancy is assumed to be sufficiently weak. Then protein concentration is mainly determined by diffusion. Thus in (1e) we neglect convective terms and we have

$$\frac{\partial \rho_1}{\partial t} \approx D_1 \nabla^2 \rho_1 . \tag{9}$$

In steady state, (9) then becomes

$$\nabla^2 \rho_1 = 0 . \tag{10}$$

Here, there is no diffusion boundary layer, so that the length scale h naturally replaces δ in (4a) and (5) leading to the results

$$\frac{\upsilon w}{h^2} \approx g \frac{\Delta \rho^s}{\rho^s}, \qquad \left(\rho_1^0 - \rho_1\right) \approx \left(\frac{\beta h}{D_1}\right)\left(\rho_1^0 - \rho_1^e\right). \tag{11a-b}$$

Using (4b) and (11b) in (11a), we find $\dfrac{\upsilon w}{h^2} \approx g \dfrac{\gamma \beta h \rho_1^0}{D_1}$, which yield

$$w \approx \frac{g \gamma \beta \rho_1^0}{\upsilon D_1} h^3. \tag{12}$$

The result given in (12) is obtained for the case of weak rotation and weak buoyancy driven flow.

3.4. Case of Moderate Rotation and Strong Buoyancy

We now consider the regime designated as moderate rotation case, where the Coriolis force dominates over the centrifugal force. This regime corresponds to

$$\Omega << \rho_1^0 \, (u^2 + v^2)^{1/2} / \rho_1, \tag{13}$$

which is determined by an order of magnitude comparison between these two forces given in (1b)-(1c).

We, thus, keep the Coriolis force plus the opposing viscous force in the non-axial components of the momentum equations (1b)-(1c) and find

$$\frac{\upsilon u}{\delta^2} \approx 2\Omega v, \frac{\upsilon v}{\delta^2} \approx 2\Omega u . \tag{14a-b}$$

For the axial component of the momentum equation (1d), we keep the buoyant force and the opposing viscous force and find

$$\frac{\upsilon w}{\delta^2} \approx g\gamma\beta \frac{\delta}{D_1}\left(\rho_1^0 - \rho_1^e\right) \approx \frac{g\gamma\beta\delta\rho_1^0}{D_1}. \tag{15}$$

From (14a-b), we find $\dfrac{u}{v} \approx \dfrac{2\Omega}{\dfrac{\upsilon}{\delta^2}} \approx \dfrac{\dfrac{\upsilon}{\delta^2}}{2\Omega}$ implying

$$2\Omega \approx \left(\frac{\upsilon}{\delta^2}\right), \; u \approx v. \tag{16a-b}$$

In addition to (13), (16a) is a second condition for the moderate rotation case. Using (16a) in (15), we find $2\Omega w \approx \dfrac{g\gamma\beta}{D_1}\left(\dfrac{\upsilon}{2\Omega}\right)^{\frac{1}{2}}\rho_1^0$, so that

$$w \approx \left[\frac{g\gamma\beta\rho_1^0}{D_1}\right]\sqrt{\nu}\left(2\Omega^{\frac{-3}{2}}\right). \tag{17}$$

The result given in (17) shows that the axial velocity reduces as the rotation rate increases.

3.5. Case of Moderate Rotation and Weak Buoyancy

Similar to the case of weak rotation and weak buoyancy presented in the sub-section 3.3, we should apply the length scale h in place of δ. Thus, here we need to replace δ in (15) by h, which lead to

$$w \approx \left(\frac{g\gamma\beta\rho_1^0}{\upsilon D_1}\right)h^3. \tag{18}$$

This result is essentially the same as the one given in (12), and the result given in (16a) is replaced by

$$2\Omega \approx \left(\frac{\upsilon}{h^2}\right). \tag{19}$$

The result given in (16b) is still valid in this case.

3.6. Case of Strong Rotation and Strong Buoyancy

Here we consider the case designated as strong rotation regime, where the centrifugal force dominates over the Coriolis force. It corresponds to the regime opposite to that given in (12) where

$$\Omega \gg \rho_1^0 \, (u^2 + v^2)^{1/2} / \rho_1, \tag{20}$$

which is determined by an order of comparison between these two forces given in (1b)- (1c). Thus, for strong rotation case, we keep the centrifugal force plus buoyant force and the opposing

viscous force in the momentum equations (1b)-(1d) and find the following estimations for the non-axial components of the flow velocity:

$$\frac{\upsilon u}{\delta^2} \approx \left[\frac{\rho_1}{\rho_1^0}\right] r\cos^2\theta\Omega^2 \,,\; \frac{\upsilon v}{\delta^2} \approx \left[\frac{\rho_1}{\rho_1^0}\right] r\cos\theta\sin\theta\Omega^2 \,,\; \frac{\upsilon w}{\delta^2} \approx g\left[\frac{\rho_1}{\rho_1^0}\right]. \tag{21a-c}$$

From (4a-b), (5) and strong buoyancy case, we have

$$\left[\frac{\rho_1}{\rho_1^0}\right] \approx \frac{\gamma\beta\delta}{D_1}\rho_1^0. \tag{22}$$

Using (22) in (21), we find

$$\frac{\upsilon u}{\delta^2} \approx \frac{\gamma\beta\delta\rho_1^0}{D_1} r\cos^2\theta\Omega^2 \,,\; \frac{\upsilon v}{\delta^2} \approx \frac{\gamma\beta\delta}{D_1}\rho_1^0 r\cos\theta\sin\theta\Omega^2 \,,\; \frac{\upsilon w}{\delta^2} \approx \frac{g\gamma\beta\delta}{D_1}\rho_1^0. \tag{23a-c}$$

Using (6) for the order of magnitude of the boundary layer thickness, we have

$$\delta^2 \approx \frac{D_1 h}{w}. \tag{24}$$

From (24) and (23), we find

$$\frac{\upsilon D_1 h}{\delta^2\delta^2} \approx \left(\frac{g\gamma\beta\rho_1^0}{D_1}\right)\delta \rightarrow \delta \approx \left(\frac{\upsilon D_1^2 h}{g\gamma\beta\rho_1^0}\right)^{\frac{1}{5}}, \tag{25a}$$

$$w \approx \frac{D_1 h}{\left(\dfrac{\upsilon D_1^2 h}{g\gamma\beta\rho_1^0}\right)^{\frac{2}{5}}} \,,\; u \approx \frac{\gamma\beta\rho_1^0}{\upsilon D_1}\left(\frac{\upsilon D_1^2 h}{g\gamma\beta\rho_1^0}\right)^{\frac{3}{5}}\Omega^2 \,,\; v \approx \frac{\gamma\beta\rho_1^0}{\upsilon D_1}\left(\frac{\upsilon D_1^2 h}{g\gamma\beta\rho_1^0}\right)^{\frac{3}{5}}\Omega^2. \tag{25b-d}$$

The results given in (25a-d) appear to be reasonable. As viscous effect increases, the boundary layer thickness increases; velocity components u, v and w decrease with increasing viscosity, and the non-axial velocity components u and v increase with the rotation rate

3.7. Case of Strong Rotation and Weak Buoyancy

Again similar to the weak buoyancy cases presented in the sub-sections 3.3 and 3.5, we need to use length scale h instead of δ. Thus, here we replace δ in (21)-(22) and (23c) by h and find

$$w \approx \left(\frac{g\gamma\beta\rho_1^0}{\upsilon D_1} \right) h^3, \tag{26a}$$

$$\frac{v}{u} \approx \tan\theta , \; u \approx (\gamma\beta\rho_1^0 \, h^2 r \, cos^2\theta \, \Omega^2)/(\nu D_1). \tag{26b-c}$$

4. Concluding Remarks

We investigated the problem of convective flow around a growing protein crystal and in the presence of an externally imposed rotational constraint. Using scaling analysis for the flow within a thin boundary layer adjacent to the crystal face, we found the following main results that are given as follows. (i) For weak rotation, where (3) holds, and strong buoyant force case, the relevant length scale is the boundary layer thickness, and the leading order viscous force balances that due to buoyancy in the axial component of the momentum equation leading to (4a). In addition, the leading order diffusion term in the concentration equation, for either protein or impurity, balances the corresponding temporal derivative term leading to a result that combined with (4a) yield (8). In this case rotational effects are insignificant. (ii) For weak rotation and weak buoyant force case, the relevant length scale is the radius of the crystal, and the similar type of balances of the forces as in the case (i) leads to (12). In this case rotational effects are again insignificant. (iii) For moderate rotation and strong buoyant force, the relevant length scale is the boundary layer thickness, and the Coriolis force in the non-axial momentum equation is significant and balances the corresponding leading order viscous force leading to (14a-b).

The leading order viscous force balances the buoyant force in the axial component of the momentum equation, which together with (14a-b) lead to the result (17). It can be seen from (17) that axial convective flow can decrease in magnitude if the rotational effect is moderate in the sense that the Coriolis force dominate over the centrifugal force. (iv) For moderate rotation and weak buoyancy case, the relevant length scale is the radius of the crystal instead of the boundary layer thickness, and the similar type of the force balances as in the case (iii) leads to (18)-(19), which imply that the axial flow decreases with increasing the rotation rate. The results for both cases of (iii) and (iv) are valid in the range where (13) and (16a) hold for the rotation rate. (v) For strong rotation and strong buoyant force, the relevant length scale is the boundary layer thickness, and the centrifugal force in the non-axial momentum equation is significant and balances the corresponding leading order viscous force leading to (21a-b). The leading order viscous force balances with the buoyant force in the axial component of the momentum equation, which leads to (21c).

The condition of strong buoyancy and the order of magnitude of the boundary layer thickness together with the results given in (21a-c) then yield (25b-d), which imply, in particular, that non-axial convective flow can be intensified if the rotational effect is strong in the sense that the centrifugal force dominates over the Coriolis force. (vi) For strong rotation and weak buoyancy case, the relevant length scale is the radius of the protein crystal, and the similar type of force balances as in the case (v) lead to (26a-c), which imply, in particular, that the non-axial flow increases with the rotation rate.

The present result about possible beneficial effect of an externally imposed rotational constraint on weakening the convective flow around a growing protein crystal and the interesting recent experimental results for the protein crystallization system and production of higher quality protein crystal in a high gravity environment [Blagova et al. (1997)] point at future useful studies of protein crystal growth on a centrifuge. It is hoped that such studies can be carried out theoretically and computationally by the first author in the near future.

Finally it should be noted that effect of a magnetic field on the growth rate of certain protein crystals, such as lysozyme and other protein crystals, has been studied experimentally in the past [Yanagiva et al. (2000), Moreno et al. (2007)], and it has been found that such effect to be notable for strong field cases. Such experimental result together with the present theoretical results for the case of convective flow during protein crystallization and those in Riahi (2001) for the case of alloy crystallization suggest that application of both a magnetic field and a rotation vector on the flow during protein crystal growth could lead to a more effective procedure to control the strength of the flow around the growing protein crystal and thereby producing higher quality protein crystal. Thus, it is also recommended future studies of convection during protein crystallization and in the presence of externally imposed rotation and magnetic field in order to detect possible relevant parameter regimes where the flow adjacent to the crystal face can be weakened as much as possible.

Acknowledgement

REFERENCES

Barenblatt, G. I. (1996). Scaling, Self-Similarity, and Intermediate Asymptotics. Cambridge University Press, UK.

Blagova, E., Mogunova, E., Smimova, A., Mikhailov, S., Armstrong, C., Mao, C. and Ealick, S. (1997). Centrifugal Materials Processing, edited by L. L. Regel and W.R. Wilcox, 203.

Cang, H-X, Wang, Y-P, Han, Y., Zhou, J-X and Bi, R-C (2003). The space experiment of protein crystallization abroad the Chinese spacecraft SZ-3. Microgravity-Science and Technology, **14**(3), 13-16.

Chandrasekhar, S. (1961). Hydrodynamic and Hydromagnetic Stability. Oxford University Press, UK.

Day, J. and McPherson, A. (1992). Macromolecular crystal growth experiments on international microgravity laboratory. Protein Science, **1**, 1254-1268.

Heijna, M. C. R., Van Enckevort, W. J. P. (2008). Growth inhibition of protein crystals: A study of Lysozyme polymorphs. Crystal Growth Research, **8**(1), 270-274.

Lee, C. P. and Chernov, A. A. (2002). Solutal convection around growing protein crystals and diffusional purification in space. Journal of Crystal Growth, **240**, 531-544.

Long, M. M., Delucas, L. J., Smith, C., Carson, M., Moore, K., Harrington, M. D., Pillion, D.J., Bishop, S.P., Rosenblum, W.M., Naumann, R.J., Chait, A., Prahl, J. and Bugg, C.E. (1994).

Protein crystal growth in microgravity-temperature induced large scale crystallization of insulin, Microgravity Science and Technology, **7**, 196-202.

Moreno, A., Quiroz-Garcia, B., Yokaichiya, F., Stojanoff V., and Rudolph, P. (2007). Protein crystal growth in gels and stationary magnetic fields, Crystal Growth and Technology, **42**(3), 231-236.

Ramachandran, N., Baugher, C.R. and Naumann R.J. (1995). Modeling flows and transport in protein crystal growth, Microgravity Science and Technology, **8**, 170-179.

Riahi, D. N. (2001). Effects of centrifugal and Coriolis forces on a hydro-magnetic chimney convection in a mushy layer, J. Crystal Growth, **226**, 393-405.

Worster, M. G. (1991). Natural convection in a mushy layer, J. Fluid Mech., **224**, 335-359.

Yanagiya, S., Sazaki, G., Durbin, S.D., Miyashita, S., Nakajima, K., Komatsu, H., Watanabe, K. and Motokawa, M. (2000). Effects of a magnetic field on the growth rate of tetragonal lysozyme crystals. J. Crystal Growth, **208**, 645-650.

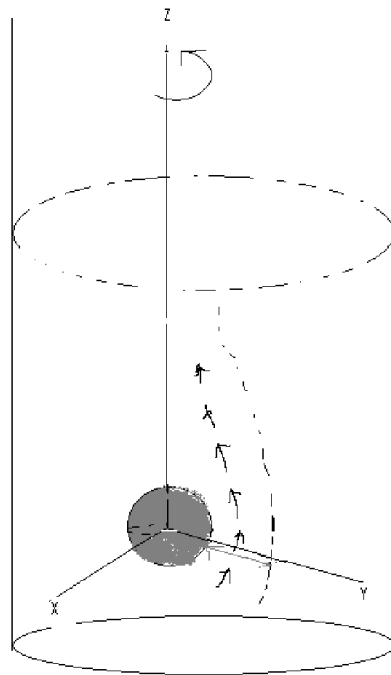Zeytounian, R.K. (2004). Asymptotic Modeling of Fluid Flow Phenomena, Springer Netherland.

Figure 1. This is a diagram for the physical system.